JACS
JOURNAL OF THE AMERICAN CHEMICAL SOCIETY

ARTICLE

pubs.acs.org/JACS

Synthesis of Fluorinated Polythienothiophene-*co*-benzodithiophenes and Effect of Fluorination on the Photovoltaic Properties

Hae Jung Son,[†] Wei Wang,[†] Tao Xu,[†] Yongye Liang,[†] Yue Wu,[‡] Gang Li,[‡] and Luping Yu*[,†]

[†]Department of Chemistry and The James Franck Institute, The University of Chicago, 929 East 57th Street, Chicago, Illinois 60637, United States

[‡]Solarmer Energy Inc., 3445 Fletcher Avenue, El Monte, California 91731, United States

Supporting Information

ABSTRACT: Herein, we describe the synthesis of fluorinated polythienothiophene-*co*-benzodithiophenes (PTBFs) and the characterization of their physical properties, especially their performance in solar cells. Fluorination of the polymer backbone lowered both the HOMO and LUMO energy levels and simultaneously widened the energy bandgap of the polymer (0.1−0.2 eV). Incorporation of fluorine into the various positions of the polymer backbone significantly affected the solar cells' power conversion efficiency from 2.3% to 7.2%. Detailed studies revealed that the polymer containing mono-fluorinated thienothiophene gave the best solar cell performance. Perfluorination of the polymer backbone led to poor compatibility with $PC_{71}BM$ molecules, thus poor solar energy conversion efficiency. This is possibly due to the enhanced self-organization properties of the polymer chains and the fluorophobicity effect. Furthermore, it was found that perfluorination of the polymer backbone resulted in poor photochemical stability against singlet oxygen attack. Theoretical studies indicated that the internal polarization caused enhancement of the negative charge density on thienothiophene rings, which rendered them vulnerable to [2+4] cycloaddition reaction with singlet oxygen.

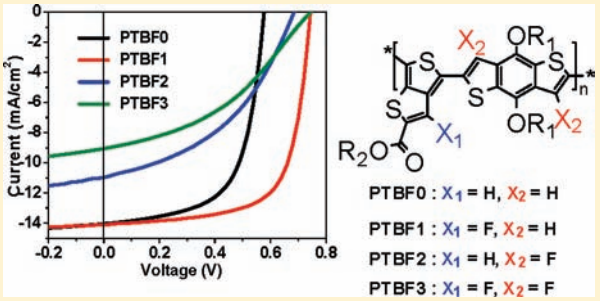

INTRODUCTION

When electron-rich conjugated polymers are blended with electron-deficient fullerene derivatives in the form of thin films, the resulting films contain high donor−acceptor interfacial areas. Once these films are placed between proper electrodes, they demonstrate the photovoltaic effect. Such devices are called polymer bulk heterojunction (BHJ) solar cells.[1,2] Polymer BHJ solar cells are viewed as promising candidates for renewable clean energy sources. Compared to inorganic solar cells, they offer advantages in preparing flexible and lightweight devices at much lower fabrication cost due to simple ambient-condition solution processing or the roll-to-roll coating process.[3,4] However, BHJ solar cells based on semiconducting polymers are complex systems; their performances are affected by many factors, e.g., the electrical properties of donor polymers, interaction of donor polymers and acceptors, morphology of the composite films, interfacial properties, and electrodes. Among these factors, the properties of semiconducting polymers play determining roles. To achieve high solar power conversion efficiency (PCE), therefore, great research efforts are focused on designing and synthesizing new polymers with improved properties.[5−14] Although the past work has generated materials with PCE close to 8%,[15] knowledge is still limited in how to further improve solar cell efficiency through polymer development. Therefore, it is necessary to carry out detailed research to elucidate the structure/property relationship. A general guideline for design of p-type polymers is a donor−acceptor alternating polymer structure, which leads to a low bandgap for efficient light harvesting. It is important that the HOMO of the donor polymers and the LUMO of acceptors match to achieve fast charge separation and high open circuit voltage (V_{oc}), thus high PCE.[16−18] Recently, our group has succeeded in developing a series of low bandgap polymers, polythieno[3,4-*b*]thiophene-*co*-benzo[1,2-*b*:4,5-*b*′]dithiophene (PTBx series),[19−21] which showed a rather synergistic combination of the desired properties, e.g., low bandgap (∼1.6 eV), relatively high mobility, proper orientation of the π-system, and controllable morphology. Introduction of a fluorine atom into the thieno[3,4-*b*]thiophene ring substantially improved the V_{oc} value, and the device achieved the highest PCE over 7%.[15,22] This improvement is mainly attributed to the lowering of the polymer HOMO energy level without significant changes in other properties. To better understand the reasons behind the high performances of these polymers and to further enhance their solar cell properties, we investigated the effects of fluorination on the properties of PTB polymers and have synthesized a series of fluorinated polymers (PTBNs) as shown in Figure 1. The original idea was to use electron-deficient fluorine atoms to further fine-tune the HOMO energy levels of the polymers. The results indicated that fluorination

Received: September 23, 2010
Published: January 25, 2011

dx.doi.org/10.1021/ja108601g | *J. Am. Chem. Soc.* 2011, 133, 1885–1894

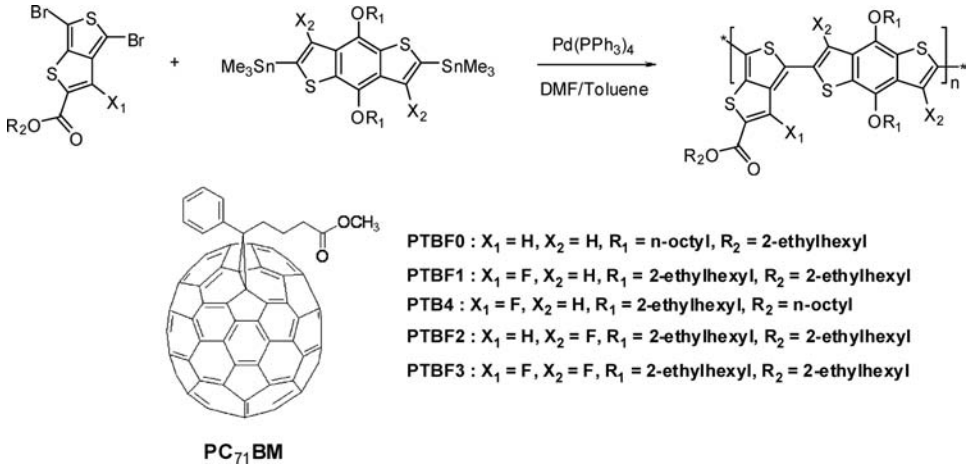

Figure 1. Synthetic routes for polymers **PTBF0**−**PTBF3** and structure of $PC_{71}BM$.

Scheme 1. Synthetic Route for Monomer 6

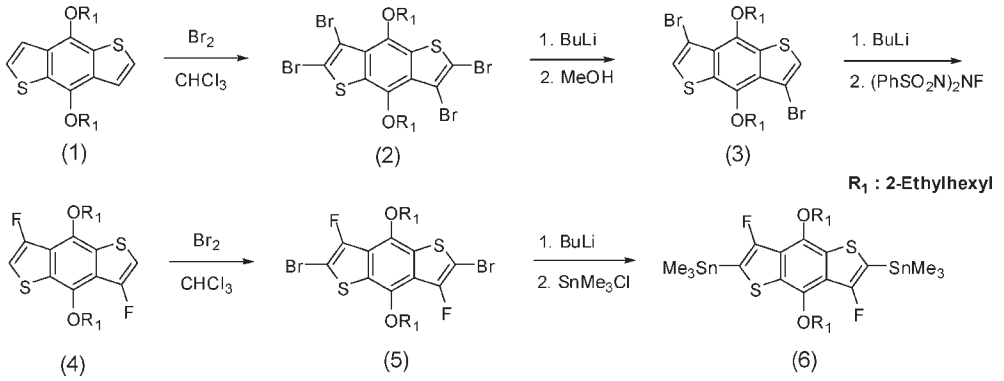

of the polymer backbone exerted an important effect not only on electronic properties but also on photochemical stability and morphological compatibility of the polymers with $PC_{71}BM$. In this paper, we describe the synthesis of new fluorinated polymers and their properties under photochemical conditions.

RESULTS AND DISCUSSION

Synthesis of Monomers and Polymers. We have synthesized four polymers for comprehensive studies, two of which are known polymers (**PTBF0** and **PTBF1**), but the solar cell properties of **PTBF0**/$PC_{71}BM$ were not reported before. To synthesize perfluorinated polymers **PTBF2** and **PTBF3**, the monomer 2,6-bis(trimethyltin)-3,7-difluoro-4,8-bis(2-ethylhexyloxy)benzo[1,2-*b*:4,5-*b*′]dithiophene (**6**) is needed, which was synthesized according to Scheme 1. First, 4,8-bis(2-ethylhexyloxy)benzo[1,2-*b*:4,5-*b*′]dithiophene was brominated at the 2, 3, 6, and 7 positions to form compound **2**; 6 equiv of bromine was used to ensure a complete reaction. Selective debromination of compound **2** at the 2 and 6 positions using lithiation and protonation led to compound **3**. The two fluorine atoms were introduced at the 3 and 7 positions of compound **3** after debromination by using *n*-butyllithium (*n*-BuLi), followed by reaction with *N*-fluorobenzenesulfonimide ($(PhSO_2)_2NF$). Compound **4** reacts with bromine to yield compound **5**, from which monomer **6** was prepared after reacting with *n*-BuLi followed by trimethyltin chloride.

This fluorination process involves an interesting and complex chemistry. In addition to compound **4**, we observed considerable amounts of compounds **7** and **8**, as shown in Scheme 2a. The formation of compounds **7** and **8** can be rationalized by taking into account the acidity of the protons next to fluorine in compound **4**. Compound **4** might be deprotonated by anion **9**, thus generating anions **10** and **11**. Mono- and tri-fluorinated compounds, **7** and **8**, could be formed after fluorination of **10** and **11** by $(PhSO_2)_2NF$. Suzuki and co-workers[23] synthesized 2,5-dibromo-3,4-difluorothiophene from 2,5-bis(trimethylsilyl)-3,4-dibromothiophene with a high yield through two-step reactions of lithiation of trimethylsilyl (TMS)-protected 3,4-dibromothiophene, followed by treatment with $(PhSO_2)_2NF$ and bromination. In order to improve the yield, we attempted to synthesize compound **5** with an approach similar to Suzuki's, as shown in Scheme 2b. In our synthesis, a *tert*-butyldimethylsilyl (TBDMS) group was used instead of a TMS group to protect the 2 and 6 positions of benzodithiophene, since desilylation of TMS was observed, most likely due to nucleophilic attack of *n*-BuLi to the silicon core. The TBDMS group is known to be stable to nucleophilic attack by *n*-BuLi and has a smaller size compared to other silane protecting groups such as the triisopropylsilyl group. Compound **12** was obtained by reacting **2** with *n*-BuLi, followed by treatment with *tert*-butyldimethylsilyl chloride under anhydrous condition. Subsequent steps of lithiation and reaction with $(PhSO_2)_2NF$ to synthesize compound **13**, to the yield **5**, failed. When the lithiated product of **12** was quenched, compounds **14**,

dx.doi.org/10.1021/ja108601g |*J. Am. Chem. Soc.* 2011, 133, 1885–1894

Scheme 2. (a) Reaction Route of the Fluorination Step, (b) Modified Reaction Scheme of Suzuki's Method, and (c) Ring-Opening Process of Compound 12

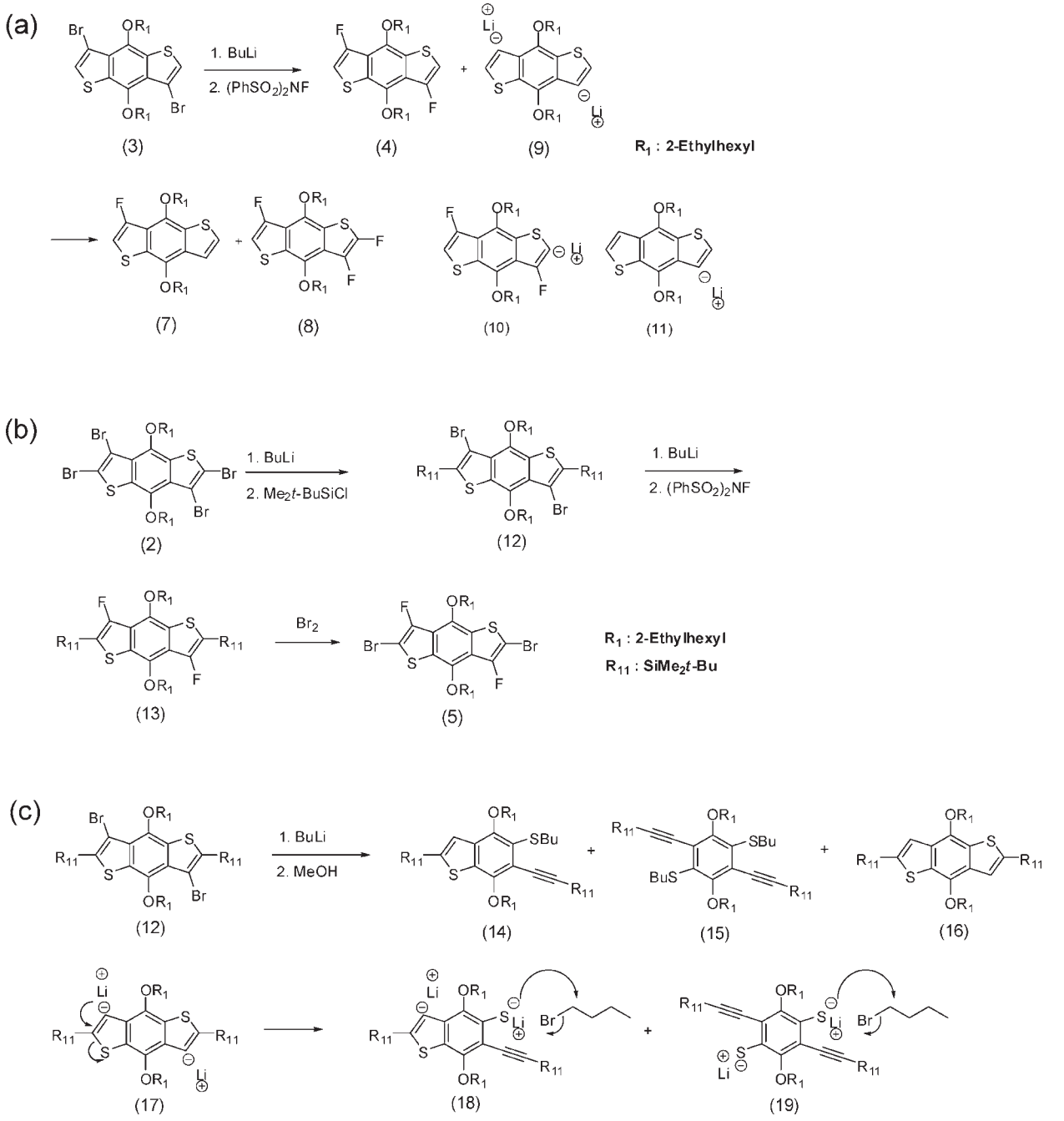

15, and **16** were found in a ratio of 1:1:1. It was thought that the anion **17** prepared by lithiation of **12** mostly underwent ring-opening processes to give the lithium salts of **18** and **19**, which reacted further via *S*-butylation with the bromobutane formed in the initial Br−Li exchange reaction (Scheme 2c). Similar results were observed in benzo[*b*]thiophen-3-yllithium and its derivatives,[24−27] which underwent a ring-opening reaction to give the lithium salt of *o*-mercaptophenylacetylenes and reacted further by *S*-butylation with bromobutane.

The polymerization was carried out via the Stille polycondensation reaction.[19] The structures of polymers were determined with ^{1}H NMR spectroscopy, which is consistent with the proposed structures. The molecular weights of the polymers were measured by using gel permeation chromatography (GPC), and the results are shown in Table 1. It was found that the polymers exhibited good solubility in many chlorinated solvents, such as chloroform and chlorobenzene. Thermogravimetric analysis (TGA) results showed that all polymers had similar thermal stability and could withstand temperatures up to about 200 °C.

Optical Properties. The UV−vis absorption spectra of the four polymer films showed two major absorption peaks as shown

dx.doi.org/10.1021/ja108601g |*J. Am. Chem. Soc.* 2011, 133, 1885–1894

Table 1. Molecular Weights and Absorption Properties of the Polymers

polymer	M_w (kg/mol)	PDI	λ_{max} (nm)	λ_{onset} (nm)	E_g^{opt} (eV)
PTBF0	23.2	1.38	683, 630	780	1.59
PTBF1	97.5	2.10	671, 628	737	1.68
PTBF2	26.7	2.38	670, 611	709	1.75
PTBF3	78.4	2.61	670, 613	717	1.73

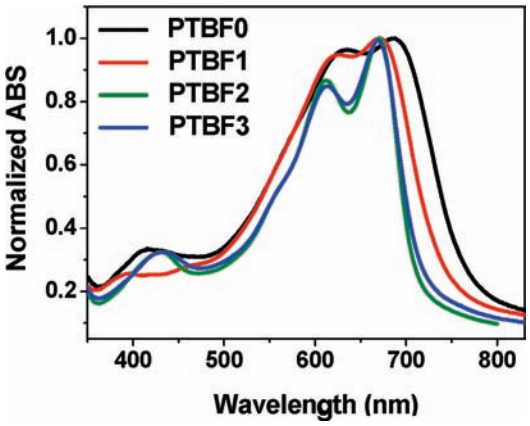

Figure 2. UV−vis absorption spectra of the polymer films.

in Figure 2. The **PTBF2** and **PTBF3** polymers exhibit sharp and clearly separated peaks, as compared with the separated but broader absorption of **PTBF0** and **PTBF1**. Introducing more electron-withdrawing groups on the polymer backbone makes the absorption onsets (λ_{onset}) and maxima (λ_{max}) of the polymers blue-shifted. For example, the λ_{onset} and λ_{max} values of **PTBF2** are ~70 nm and 10−20 nm blue-shifted from those of **PTBF0**, respectively. This leads to widening in the energy bandgap, as shown in Table 1. A similar effect was reported in a fluorine-substituted thiophene oligomer.[23] Tetradecafluorosexithiophene showed onset and maximum absorption shifted to higher energies relative to those of unfluorinated sexithiophene. The blue shift of λ_{onset} of **PTBF1** compared to **PTBF0** can also be partly attributed to the structural change of the alkyl side chain from *n*-octyl for **PTBF0** to 2-ethylhexyl for **PTBF1**. Bulkier side chains in polymers lead to longer polymer interchain distances and hence reduce the backbone interchain interaction. This results in a change in the polymer chain packing in the film and the blue-shifted absorption.[28] The absorption spectra of **PTBF2** and **PTBF3** are very similar, indicating that further substitution of fluorine to the backbone of **PTBF2** does not change its optical properties significantly. The spectroscopic data of the polymers are summarized in Table 1, where the optical bandgap (E_g^{opt}) of the four polymers was determined from the onset of absorption (λ_{onset}).

Electrochemical Properties. Electrochemical properties of the polymers were investigated by using cyclic voltammetry (CV). The HOMO and LUMO energy levels of the four polymers were deduced from their voltammograms and are shown in Figure 3. The results reveal that introduction of fluorine to thienothiophene or benzodithiophene in the polymer backbone reduces both HOMO and LUMO energy levels, although the energy levels for **PTBF2** and **PTBF3** are very similar. The electrochemical bandgap (E_g^{cv}) of the four polymers, calculated from the difference between HOMO and LUMO values, however,

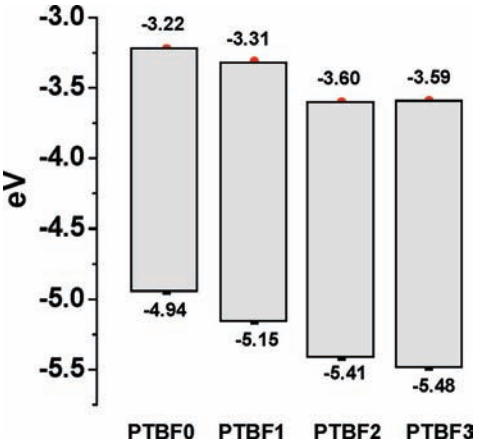

Figure 3. HOMO and LUMO energy levels of the polymers.

consistently yielded larger values than the optical bandgap by ΔE = 0.06−0.16 eV. The difference is caused by the fact that redox potentials are determined by the energy used for electron addition and extraction, for which Coulombic attraction must be accounted, whereas the optical band gap is the energetic difference between the ground and the excited states.

Theoretical Calculation. To predict the electronic properties and energy levels, theoretical calculations were performed by using the density functional theory (DFT) with the B3LYP/6-31G* basis set.[29] To make computation possible, we chose several repeating units as simplified models. The frontier molecular orbitals and optimized molecular geometries are illustrated in Figure 4. The dihedral angles between the units of thieno[3,4-*b*]thiophene and benzo[1,2-*b*:4,5-*b*′]dithiophene of these four oligomers are summarized in Table 2. Fluorinated oligomers favor planar conformation. For instance, the dihedral angles of **PTBF2** and **PTBF3** are close to 180°. Theoretical and experimental studies of oligothiophene[23,30,31] showed that inter- and intra-ring single bond lengths become shortened upon fluorination, suggesting that the conjugation is increased in the oligothiophene, especially between rings. Likewise, fluorination of the oligomer backbone might increase the conjugation in **PTBF2** and **PTBF3**, contributing to the planar conformation of the **PTBF2** and **PTBF3** oligomers. As is shown in Figure 4, the distributions of HOMO wave functions in these four oligomers are similar to a certain degree. All of the HOMO wave functions delocalize over the whole π-conjugated systems. However, a clear trend is visible when comparing the LUMO wave functions of **PTBF0**, **PTBF1**, **PTBF2**, and **PTBF3**: the introduction of fluorine atoms leads to a more delocalized LUMO wave function. This trend is in agreement with the planar molecular geometries adopted by fluorinated oligomers.

X-ray Analysis. To probe the structural order, X-ray diffraction analyses on polymer films were performed (Figure 5). All four polymers commonly showed two diffraction peaks at about 22.8−24° and 4.2−4.8°. These refraction values are similar to those reported for PTB1 and other conjugated polymers.[32−34] The reflection at 22.8−24° (corresponding to a distance of ~3.8−4 Å) is a typical π-stacking spacing of conjugated polymer backbones, and the other peak at 4.2−4.8° (~28−31 Å) may be related to the spacing between coplanar alkyl chains (Table 3). **PTBF0** shows the shortest π-stacking spacing, which is most likely due to the less bulky *n*-octyl side chain grafted onto benzodithiophene of the polymer backbone, compared to the

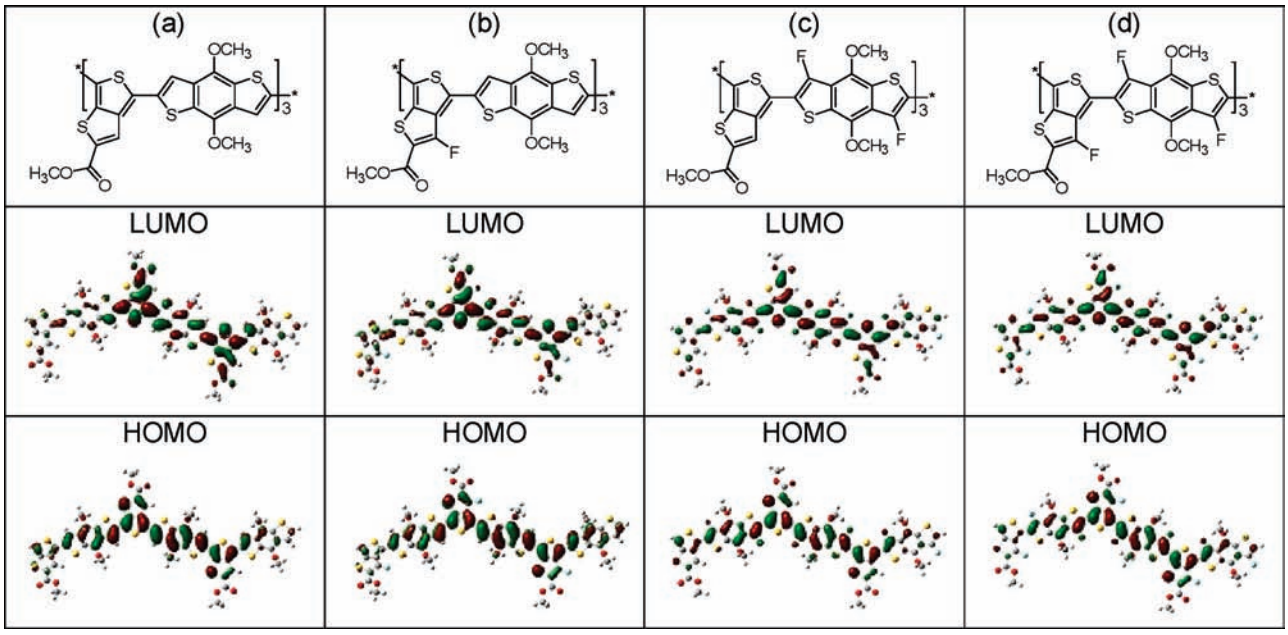

Figure 4. HOMO and LUMO of the oligomers at the B3LYP/6-31G* level of theory: (a) **PTBF0**, (b) **PTBF1**, (c) **PTBF2**, and (d) **PTBF3**.

Table 2. Calculated Values of Dihedral Angles of the Polymers

polymer	dihedral angle (deg)
PTBF0	163.3
PTBF1	161.0
PTBF2	179.5
PTBF3	179.8

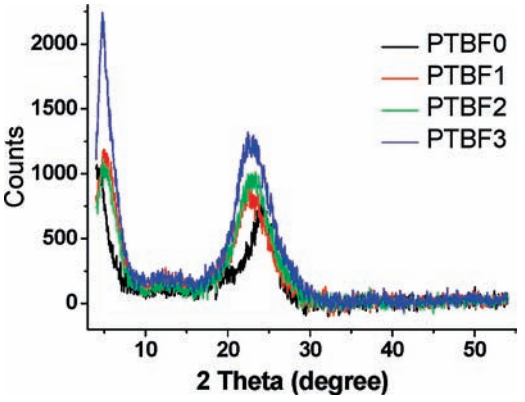

Figure 5. X-ray diffraction patterns of the polymer films.

other polymers including a bulky branched side chain on the same unit. In contrast, the spacing between coplanar alkyl chains of **PTBF0** is 2−3 Å longer than those of the other polymers because of the longer chain length of linear octyl relative to a branched octyl side chain. As more fluorine atoms are introduced on the polymer backbone, the polymer presents more pronounced reflection, indicating a higher structural organization in the solid state. **PTBF3** exhibits sharper features compared to the other three polymers, suggesting it possesses the highest crystalline structure. The characteristic changes in the polymer organization can be explained by the calculated results of the oligomers' optimized conformation corresponding to the four

Table 3. *d*-Spacing Values of the Polymers

polymer	*d*1 (Å)	*d*2 (Å)
PTBF0	3.8	31
PTBF1	4.0	28
PTBF2	4.0	29
PTBF3	4.0	28

polymers. The dihedral angles of oligomers increase from **PTBF0** to **PTBF3**, and this result rationalizes the improved crystallinity of the polymer films since the high molecular planarity is favorable for the regular arrangement of the polymer chains.[10] A certain degree of intermolecular interactions might be aroused by fluorine substitution of an aromatic polymer backbone (e.g., the interaction between an electron-rich aromatic ring and an electron-deficient fluororinated aromatic ring) and contribute to the increased crystalline structure in the polymer film.[35] More detailed structural studies using GISAXD are in progress and will be reported at a later date.

Solar Cell Performance. The photovoltaic properties of the polymers were studied in solar cells with structures of ITO/PEDOT:PSS/polymer:$PC_{71}BM$/Ca/Al. The active layers were spin-coated from 1,2-dichlorobenzene (DCB) solutions of the polymers and $PC_{71}BM$, and the optimized weight ratios of polymer to $PC_{71}BM$ were 1:1, 1:1.5, 1:1.5, and 1:1.5 for **PTBF0**, **PTBF1**, **PTBF2**, and **PTBF3**, respectively. Figure 6a shows the curves of current density versus voltage ($I-V$), measured under AM 1.5 condition at 100 mW/cm^2. The representative characteristics of the solar cells are summarized in Table 4. It is interesting to note that **PTBF0** and **PTBF1** exhibit much better solar cell performances compared to the solar cells made of **PTBF2** and **PTBF3**.

Among all photovoltaic parameters measured, the most remarkable difference observed was in the fill factor (FF). Although **PTBF2** has a similar molecular weight to **PTBF0** and the same backbone structure except for the fluorine substitution in benzodithiophene, the FF of **PTBF0** is ∼50% higher than that of

dx.doi.org/10.1021/ja108601g |*J. Am. Chem. Soc.* 2011, 133, 1885–1894

PTBF2. **PTBF3** showed the lowest FF among all polymers, with a value ~30% smaller than that of **PTBF1**, which has comparable structure and molecular weight. The short-circuit current density (J_{sc}) values of **PTBF0** and **PTBF1** are also 3−4 mA/cm^2 higher than those of **PTBF2** and **PTBF3**. **PTBF0** and **PTBF1** showed similar J_{sc} and FF, although the PCE of **PTBF1** is higher than that of **PTBF0** due to an enhanced open circuit voltage (V_{oc}). In our previous results,[19,22] the solar cell performance of the fluorinated PTB polymers was improved by using the mixed solvent of 97% DCB/3% 1,8-diiodoctane (DIO) to form the active layer. Therefore, we repeated the solar cell test for **PTBF1**, **PTBF2**, and **PTBF3** both with and without the 3% DIO additive. **PTBF1** exhibited improved performance in both J_{sc} and FF, resulting in a maximum efficiency of 7.2%. In contrast, the J_{sc} and FF of **PTBF2** and **PTBF3** became slightly worse. In the case of **PTBF3**, the V_{oc} was also decreased compared with that of the first test (Figure 6). Because the structure of the polymer side chain is reported as one of the important variables that affect solar cell properties,[10,36−38] we investigated the solar cell properties of **PTB4**,[19] of which an *n*-octyl side chain in thienothiophene is modified from 2-ethylhexyl in **PTBF1**. With the same device structure and fabrication condition (97% DCB/3% DIO solvent) as **PTBF1**, the optimized composition of **PTB4** with $PC_{71}BM$ is 1:1. Compared to **PTBF1**, J_{sc} of **PTB4** is slightly higher (14.8 mA/cm^2 vs 14.1 mA/cm^2), but FF is reduced (64.6% vs 68.9%). The solar cell PCE of **PTB4** is 6.7% (7.0% after spectral correction), which is comparable to that of **PTBF1**. On the basis of comparisons of the solar cell results for **PTBF1**, **PTBF3**, and **PTB4**, we conclude that the fluorine substitution has a more substantial influence on polymer solar cell properties than the structural modification of the polymer side chain.

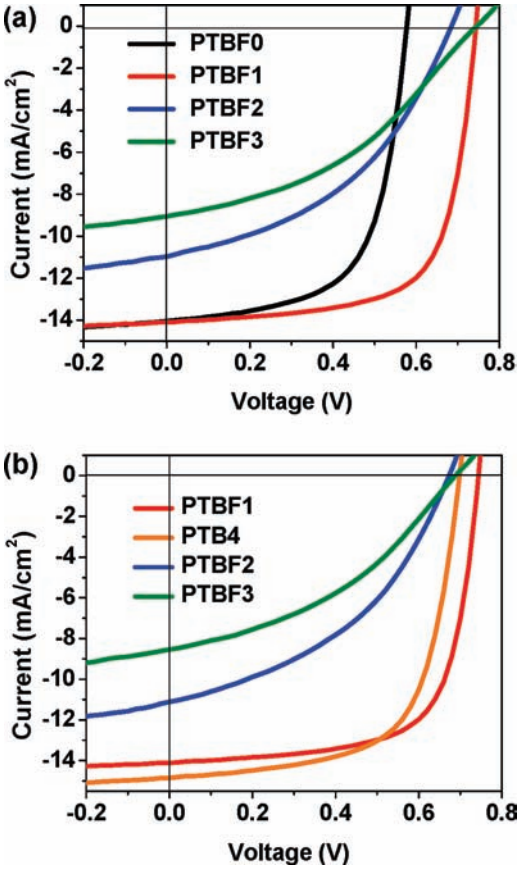

Figure 6. *I*−*V* curves of solar cells prepared with solvent DCB (a) and mixed solvent 97% DCB/3% DIO (b).

Since the photocurrent is mostly limited by photoinduced charge carrier generation and transport, the nanoscale morphology of the polymer/PCBM blend film is an important factor for determining the values of J_{sc} and FF. In order to analyze the correlation between the polymer structure and solar cell properties, we investigated the morphology of polymer/$PC_{71}BM$ blend films using transmission electron microscopy (TEM). Figure 7 shows TEM images of polymer/$PC_{71}BM$ blend films prepared using the same conditions as those for the formation of the solar cell active layers. Both TEM images of **PTBF0** and **PTBF1** blend films possess uniform and fine features, suggesting nanoscale phase separation. However, the TEM images of **PTBF2** and **PTBF3** blend films clearly show spherical domains with a size of 50−200 nm, indicating large-scale phase separation and no bicontinuous networks. Since the $PC_{71}BM$ exhibits a higher electron density than PTBF polymers, it scatters electrons more efficiently from the electronic beam.[9] The dark regions in the TEM images are attributed to $PC_{71}BM$-rich domains and the bright regions to the polymer-rich domains. Due to the limited diffusion length of excitons (10 nm), which is much smaller than the large features (50−200 nm) seen in the blend film images of **PTBF2** and **PTBF3**, photogenerated excitons will mainly recombine before reaching the interfaces of the donor and acceptor, resulting in reduced charge carrier generation and a concomitant loss of photocurrent. The nonoptimized morphology can reduce hole or electron drift length (or both of holes and electrons). The space charge accumulation caused by sluggish charge carriers subsequently induces a nonuniform electric field, which gives rise to a decreased photocurrent with strong electric field dependence, resulting in low FF.[39] The difference in morphology of the different polymer blends with $PC_{71}BM$ correlated with crystallinity of the polymers in the solid state.

Table 4. Characteristic Properties of Polymer Solar Cells

polymer	polymer/PCBM (w/w ratio)	solvent	J_{sc} (mA/cm^2)	V_{oc} (V)	FF (%)	PCE (%)
PTBF0	1:1	DCB	14.1	0.58	62.4	5.1(5.3[b])
PTBF1	1:1.5	DCB	14.0	0.74	60.3	6.2[a]
PTBF1	1:1.5	DCB/DIO	14.1	0.74	68.9	7.2[a]
PTB4	1:1	DCB/DIO	14.8	0.70	64.6	6.7(7.0[b])
PTBF2	1:1.5	DCB	11.0	0.68	43.4	3.2(3.3[b])
PTBF2	1:1.5	DCB/DIO	11.1	0.68	42.2	3.2(3.3[b])
PTBF3	1:1.5	DCB	9.1	0.75	39.4	2.7(2.8[b])
PTBF3	1:1.5	DCB/DIO	8.8	0.68	39.0	2.3(2.4[b])

[a] Data from ref 22. [b] Value after spectral correction; a spectral mismatch factor of 0.96 was calculated according to ref 61.

dx.doi.org/10.1021/ja108601g |*J. Am. Chem. Soc.* 2011, 133, 1885–1894

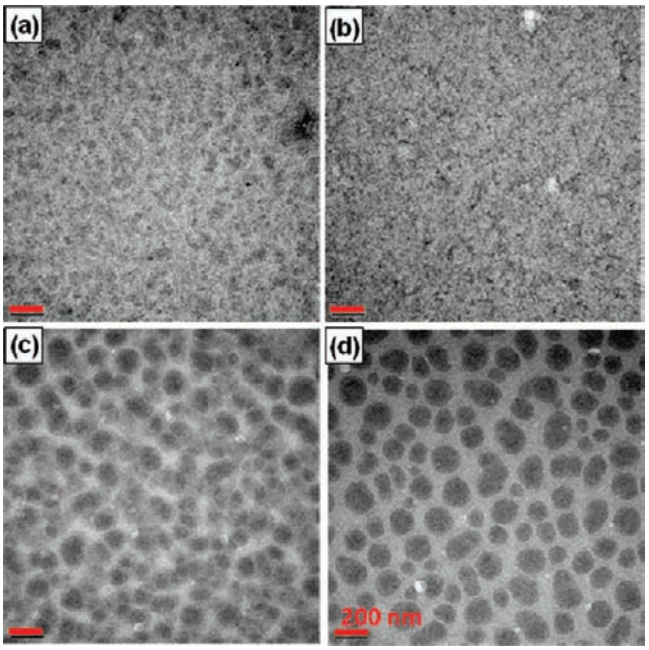

Figure 7. TEM images of polymer/$PC_{71}BM$ blend films prepared from DCB solvent: **PTBF0** (a), **PTBF1** (b), **PTBF2** (c), and **PTBF3** (d). Scale bar = 200 nm.

The strong driving force for the development of long-range order aided by the planarity of the polymer backbone favors the exclusion of the fullerene and induces a large extent of phase segregation in a blend film with the fullerene.[40] The fluorinated backbones introduce fluorophobicity for $PC_{71}BM$ molecules, a further driving force for phase separation.

The charge-carrier mobility of these polymers was measured by using the space-charge-limited current (SCLC) method in the direction perpendicular to the electrodes. For pure **PTBF0**, **PTBF1**, **PTBF2**, and **PTBF3**, the SCLC mobilities were measured to be 2.7×10^{-4}, 4.1×10^{-4}, 1.8×10^{-4}, and 7.0×10^{-5} $cm^2\ V^{-1}\ s^{-1}$, respectively. Although the mobility of **PTBF2** is slightly lower compared with **PTBF0** and **PTBF1**, the mobilities for **PTBF0**, **PTBF1**, and **PTBF2** have the same order of magnitude, but **PTBF3**, with the highest degree of crystallinity, has the lowest mobility among the four polymers. This result is not unusual since factors other than film crystallinity can influence polymer mobility (i.e., the molecular weight and polydispersity of the polymer, interconnection between neighboring phase, the domain boundary structure, and defects in the polymer film).[41−43]

From these results, it is clear that the dramatic decrease of the FF observed in P**TBF2**/$PC_{71}BM$ and **PTBF3**/$PC_{71}BM$ photovoltaic devices is mostly due to the morphology problem coming from poor miscibility of the polymers with $PC_{71}BM$. The smaller mobility also contributed to the decrease. It can be expected that if $PC_{71}BM$ molecules with better miscibility with fluorinated polymers are used, the solar cell efficiency should be improved. Our next research effort is directed toward addressing this issue.

The fluorinated polymer (**PTBF1**, **PTB4**, **PTBF2**, and **PTBF3**) devices showed enhanced V_{oc} compared with the non-fluorinated polymer, **PTBF0**, which is expected from the HOMO energy level differences. In spite of the lower HOMO energy levels of **PTBF2** and **PTBF3**, however, the overall V_{oc} values of **PTBF2** and **PTBF3** are lower than that of **PTBF1**. For both polymers of **PTBF2** and **PTBF3**, $I-V$ curves of the solar cells exhibit slopes at zero voltage, which indicates reduced parallel resistance (R_p). The observed V_{oc} decrease for **PTBF2** and **PTBF3** might be caused by a reduced shunt.[44,45] It was reported that poor film quality, such as formation of large PCBM aggregation, is detrimental to the interfacial structure between the organic active layer and the electrode and makes continuous conducting paths of the donor or acceptor between two electrodes, which results in reduced R_p and low V_{oc}.[46−48] Another factor contributing to low V_{oc} is the increased bimolecular recombinations caused by the absence of a nanoscale percolating network in **PTBF2** and **PTBF3** blend films, as shown by many past studies which showed that bimolecular recombination dynamics limited V_{oc} values.[49−52]

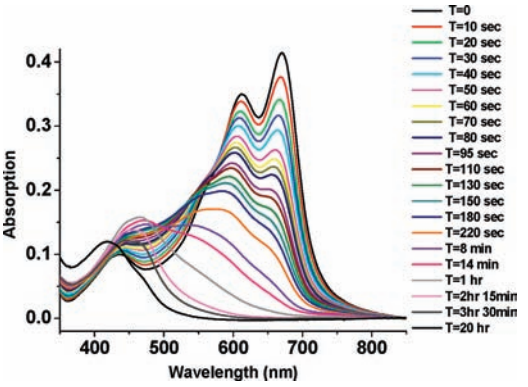

Figure 8. Absorption spectra of **PTBF3** film recorded as a function of irradiation time under air.

Photochemical Stabilities of Polymers. An interesting observation is that the **PTBF2** and **PTBF3** polymers are photochemically much more unstable compared to **PTBF0** and **PTBF1** under ambient atmosphere. With UV light exposure to the spin-coated polymer films in air, the maximum absorption peaks of the **PTBF2** and **PTBF3** polymers at 670 nm decreased in intensity, and a blue shift was observed. When the **PTBF3** film was exposed to UV light in vacuum (10^{-1} Torr), after exposure for 12 h, the UV−vis absorption spectrum was measured and compared with the initial absorption. The result showed that the initial maximum and optical density of the UV−vis absorption for the film were almost completely conserved. The film kept in the dark exposed to air exhibited almost no change in the optical density of the absorption for 12 h. This was in drastic contrast to the film exposed to UV light in air, which showed a dramatic decrease in the optical density of the maximum absorption. In this sample, the absorption amplitude at 670 nm was reduced to approximately half after 2 min. The **PTBF2** polymer showed similar results from the same experiments. In the case of **PTBF0** and **PTBF1**, it took more than 9 h for the optical density of λ_{max} to be reduced to half under the same conditions of UV light and air. These results suggest that the decomposition caused in the polymers is due to photooxidation, which occurs much more significantly to **PTBF2** and **PTBF3** (Figures 8 and 9). Photodegradation of the polymers was also observed in the solution state. The absorption spectra of toluene solutions of **PTBF2** and **PTBF3** after photodegradation were very similar to those recorded from **PTBF2** and **PTBF3** films. IR spectra of the polymers after photodegradation in the solution and the solid states were not different from each other. Therefore, photodegradation of **PTBF2** and **PTBF3** is considered to occur through the same mechanism both in the solution and in the solid state.

dx.doi.org/10.1021/ja108601g |*J. Am. Chem. Soc.* 2011, 133, 1885–1894

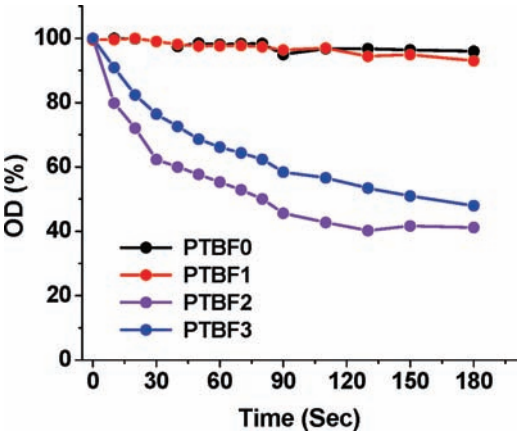

Figure 9. Decrease in the optical density (λ_{max}) of polymer films.

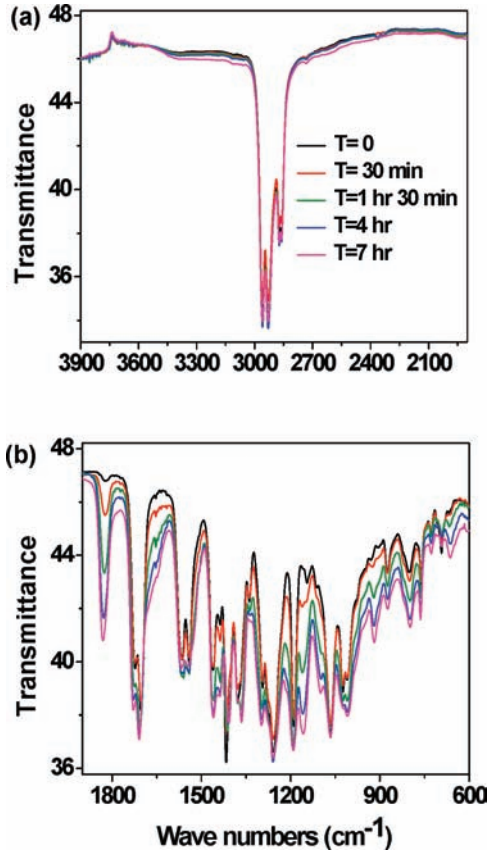

Figure 10. FT-IR of **PTBF3** film on KBr as a function of time of irradiation.

In order to gain more insight into this process, we monitored the photochemical reaction of the **PTBF3** film by using an FT-IR spectrometer. The aliphatic C−H stretching peaks in the region 2900 cm^{-1} were almost conserved after 7 h irradiation, indicating that alkyl side chains in the polymer did not participate in the photochemical reaction (Figure 10a). Evolution of a strong and complex band at 1600−1800 cm^{-1} after UV light exposure is ascribed to the C═O group (Figure 10b). Formation of strong bands in the region 1000−1200 cm^{-1} indicates sulfine residues of the structure C═$S^{+}O^{-}$ or C═S═O. The 920 cm^{-1} band, which is attributed to the C−O group, is also observed. These

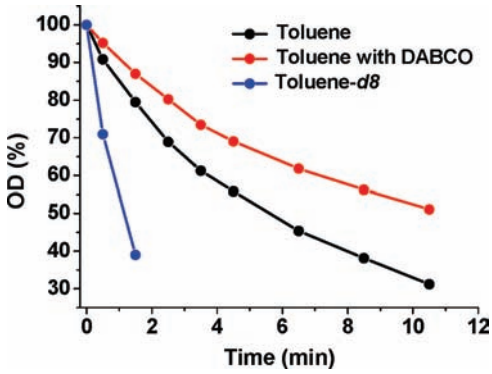

Figure 11. Optical density (%) of **PTBF3** absorption in three different systems as a function of elapsed photolysis time. For all three systems, the absorption at $T = 0$ was 1.84 ([PTBF3] ≈ 1 mg/20 mL), and [DABCO] was 4.46 × 10^{-2} M.

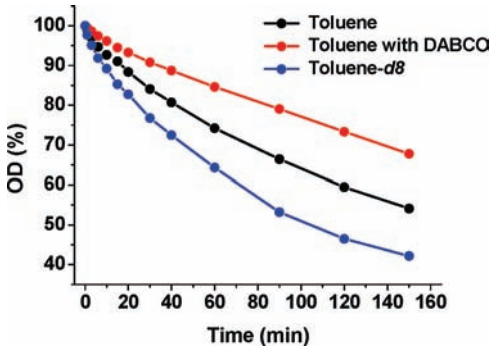

Figure 12. Optical density (%) of **PTBF1** absorption as a function of elapsed photolysis time. For all three systems, the absorption at $T = 0$ was 2.44 ([PTBF1] ≈ 1 mg/20 mL), and [DABCO] was 4.46 × 10^{-2} M.

results suggest that the thiophene ring is the core of the photochemical reaction. For the purpose of comparison, we synthesized an oligomer of **PTBF3** (M_n = 5.7K) and monitored the chemical shifts of the exposed oligomer using ^{19}F NMR spectroscopy. Since the peaks of fluorine in the different magnetic environments caused by the various lengths of oligomer chains are indicated together, it is difficult to assign all the peaks in the ^{19}F NMR spectrum. The spectrum, however, shows that all peaks still appear in the region corresponding to aromatic or vinylic fluorine (^{19}F NMR ($CDCl_3$): δ 109−129) after the photooxidation. Therefore, it is expected that the conjugation of the fluorine-substituted thiophene ring is not destroyed after the photochemical reaction. In the thienothiophene of the oligomer backbone, the thienyl ring directly linked to the polymer main chain is most likely to be the reaction site.

The photooxidation mechanism of P3HT was reported previously, which is attributed to the generation of singlet oxygen by energy transfer from the photoexcited P3HT to the triplet oxygen and subsequent reaction of the singlet oxygen with the thienyl moieties by [2+4] cycloaddition.[53,54] A similar mechanism can be postulated for the photodegradation of **PTBF3**.

The results of the following experiments imply the involvement of singlet oxygen in photodegradation of **PTBF3**: (1) Upon UV light irradiation of an aerated deuteriotoluene (toluene-d_8) solution containing **PTBF3**, the decrease rate of the optical density at 670 nm was approximately 3 times faster than that observed in toluene-h_8. Singlet oxygen lifetime in toluene-d_8 (264 μs) is longer

dx.doi.org/10.1021/ja108601g |J. Am. Chem. Soc. 2011, 133, 1885–1894

Table 5. Negative Charges on the Atom Positions A and B

Position	PTBF0	PTBF1	PTBF2	PTBF3
A (●)	-0.209	-0.214	-0.217	-0.221
B (●)	-0.239	-0.234	-0.250	-0.249

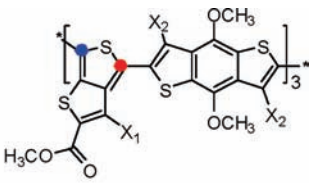

PTBF0 : X_1 = H, X_2 = H
PTBF1 : X_1 = F, X_2 = H
PTBF2 : X_1 = H, X_2 = F
PTBF3 : X_1 = F, X_2 = F

than that in toluene-h_8 (30.3 μs).[55] (2) The rate of the UV absorption changes observed on irradiation of the aerated **PTBF3** solution was reduced by the addition of a singlet oxygen quencher, 1,4-diazobicyclo[2.2.2]octane (DABCO),[56,57] as shown in Figure 11. These data show that the photodegradation rate of **PTBF3** is dependent on the lifetime of the singlet oxygen in the polymer solution. Among three tested solutions, singlet oxygen can survive the longest in toluene-d_8. In toluene with DABCO, the lifetime of singlet oxygen is the shortest. The stability of **PTBF3** from photodegradation is increased in the DABCO/toluene solution compared to the toluene-d_8 solution. For the purpose of comparison, the same experiments were carried out with **PTBF1**, which has a similar M_w value and the same structure of thienothiophene on the polymer backbone. The results in Figure 12 show that **PTBF1** also underwent photodegradation; however, the reaction rate was much slower than for **PTBF3**.

The observation that **PTBF0** and **PTBF1** are photochemically more stable than **PTBF2** and **PTBF3** is interesting and warrants more discussion. It was reported that the cycloaddition of singlet oxygen is controlled by energy matching of the frontier molecular orbitals.[58] Since singlet oxygen has a HOMO energy level of −10.73 eV and LUMO −0.98 eV,[58] the most likely addition would occur from the HOMO of the polymer and the LUMO from singlet oxygen. In accordance, we would expect that **PTBF0** and **PTBF1** would be more reactive than the other two polymers because their HOMO energy levels are closer to the LUMO of singlet oxygen. However, molecular orbital calculations provided an alternate explanation. The molecular orbitals of the HOMO were more localized on the 4 and 6 positions in the thienothiophene unit. Their charge distributions were calculated to be negative, favoring [2+4] cycloaddition reactions. As shown in Table 5, in **PTBF0** and **PTBF1**, the A and B positions in thienothiophene units are less electron-rich than those in **PTBF2** and **PTBF3**. Since singlet oxygen is an electron-deficient dienophile, it reacts more easily with a diene that contains higher electron density[59,60] Therefore, it can be assumed that the thienothiophene unit bearing higher density of negative charge at the A and B positions is more reactive toward [2+4] cycloaddition with singlet oxygen than those with less charged or neutral moieties.

In **PTBF0** and **PTBF1**, the electron-withdrawing group on the thienothiophene unit pulls the electron density out of the ring and diminishes the negative charge at the A and B positions. When the benzodithiophene unit is substituted with fluorine atoms, electron density in the thienothiophene unit would be pulled back to the A and B positions, which makes these positions more sensitive toward singlet oxygen attack.

CONCLUSION

In this study, several important points can be deduced. First, modification by fluorination on the polymer backbone can have a significant effect on the physical properties of polymers, ranging from crystallinity, energy level, internal polarization, and photochemical stability. Incorporation of fluorine is effective to control the HOMO and LUMO energy levels without a large change in the energy bandgap. Second, mutual compatibility of the donor polymer and fullerene derivative acceptor can dramatically affect the solar cell power output. In this work, fluorination provides the driving force for the phase separation of the polymer/$PC_{71}BM$ blend film, resulting in a big difference in solar cell efficiency among the polymers. Third, internal polarization is important to stabilize polymers against singlet oxygen attack, which is related to the charge density distribution at specific thiophene rings. Fourth, to enhance solar cell performances, a synergistic optimization of the polymer structure is crucial. As the polymer structure changes, the structure of acceptors should also be tuned.

ASSOCIATED CONTENT

Supporting Information. Synthesis, electrochemical studies, hole mobility measurement, photodegradation experiment, device preparation and characterization, XRD measurement and *d*-spacing values, and TEM measurement. This material is available free of charge via the Internet at http://pubs.acs.org.

AUTHOR INFORMATION

Corresponding Author
lupingyu@uchicago.edu

ACKNOWLEDGMENT

The authors acknowledge financial support from NSF, AFOSR, and NSF-MRSEC. The works described here were also partially supported by Solarmer Energy Inc. and Intel.

REFERENCES

(1) Skotheim, T. A.; Reynolds, J. *Handbook of conducting polymers*; CRC: London, 2007.
(2) Yu, G.; Gao, J.; Hummelen, J. C.; Wudl, F.; Heeger, A. J. *Science* **1995**, *270*, 1789.
(3) Gunes, S.; Neugebauer, H.; Sariciftci Niyazi, S. *Chem. Rev.* **2007**, *107*, 1324.

(4) Spanggaard, H.; Krebs, F. C. *Sol. Energy Mater. Sol. Cells* **2004**, *83*, 125.
(5) Cheng, Y.-J.; Yang, S.-H.; Hsu, C.-S. *Chem. Rev.* **2009**, *109*, 5868.
(6) Chen, J.; Cao, Y. *Acc. Chem. Res.* **2009**, *42*, 1709.
(7) Kroon, R.; Lenes, M.; Hummelen, J. C.; Blom, P. W. M.; de Boer, B. *Polym. Rev.* **2008**, *48*, 531.
(8) Peet, J.; Kim, J. Y.; Coates, N. E.; Ma, W. L.; Moses, D.; Heeger, A. J.; Bazan, G. C. *Nat. Mater.* **2007**, *6*, 497.
(9) Park, S. H.; Roy, A.; Beaupre, S.; Cho, S.; Coates, N.; Moon, J. S.; Moses, D.; Leclerc, M.; Lee, K.; Heeger, A. J. *Nat. Photon.* **2009**, *3*, 297.
(10) Piliego, C.; Holcombe, T. W.; Douglas, J. D.; Woo, C. H.; Beaujuge, P. M.; Frechet, J. M. J. *J. Am. Chem. Soc.* **2010**, *132*, 7595.
(11) Wang, E.; Wang, L.; Lan, L.; Luo, C.; Zhuang, W.; Peng, J.; Cao, Y. *Appl. Phys. Lett.* **2008**, *92*, 033307/1.
(12) Hou, J.; Chen, H.-Y.; Zhang, S.; Li, G.; Yang, Y. *J. Am. Chem. Soc.* **2008**, *130*, 16144.
(13) Zheng, Q.; Jung, B. J.; Sun, J.; Katz, H. E. *J. Am. Chem. Soc.* **2010**, *132*, 5394.
(14) Campoy-Quiles, M.; Ferenczi, T.; Agostinelli, T.; Etchegoin Pablo, G.; Kim, Y.; Anthopoulos Thomas, D.; Stavrinou Paul, N.; Bradley Donal, D. C.; Nelson, J. *Nat. Mater.* **2008**, *7*, 158.
(15) Chen, H.-Y.; Hou, J.; Zhang, S.; Liang, Y.; Yang, G.; Yang, Y.; Yu, L.; Wu, Y.; Li, G. *Nat. Photon.* **2009**, *3*, 649.
(16) Thompson, B. C.; Frechet, J. M. J. *Angew. Chem., Int. Ed.* **2008**, *47*, 58.
(17) Bundgaard, E.; Krebs, F. C. *Sol. Energy Mater. Sol. Cells* **2007**, *91*, 954.
(18) Roncali, J. *Macromol. Rapid Commun.* **2007**, *28*, 1761.
(19) Liang, Y.; Feng, D.; Wu, Y.; Tsai, S.-T.; Li, G.; Ray, C.; Yu, L. *J. Am. Chem. Soc.* **2009**, *131*, 7792.
(20) Liang, Y.; Wu, Y.; Feng, D.; Tsai, S.-T.; Son, H.-J.; Li, G.; Yu, L. *J. Am. Chem. Soc.* **2009**, *131*, 56.
(21) Liang, Y.; Yu, L. *Acc. Chem. Res.* **2010**, *43*, 1227.
(22) Liang, Y.; Xu, Z.; Xia, J.; Tsai, S.-T.; Wu, Y.; Li, G.; Ray, C.; Yu, L. *Adv. Mater.* **2010**, *22*, E135.
(23) Sakamoto, Y.; Komatsu, S.; Suzuki, T. *J. Am. Chem. Soc.* **2001**, *123*, 4643.
(24) Iddon, B.; Dickinson, R. P. *J. Chem. Soc. C* **1970**, 2592.
(25) Dickinson, R. P.; Iddon, B. *Tetrahedron Lett.* **1970**, 975.
(26) Dickinson, R. P.; Iddon, B. *J. Chem. Soc. C* **1971**, 3447.
(27) Fuller, L. S.; Iddon, B.; Smith, K. A. *Chem. Commun.* **1997**, 2355.
(28) Theander, M.; Inganaes, O.; Mammo, W.; Olinga, T.; Svensson, M.; Andersson, M. R. *J. Phys. Chem. B* **1999**, *103*, 7771.
(29) Parr, R. G.; Weitao, Y. *Density Functional Theory of Atoms and Molecules*; Oxford University Press: New York, 1989.
(30) Sakamoto, Y.; Komatsu, S.; Suzuki, T. *Synth. Met.* **2003**, *133*−*134*, 361.
(31) Salzner, U. *J. Phys. Chem. A* **2010**, *114*, 5397.
(32) Chabinyc, M. L. *Polym. Rev.* **2008**, *48*, 463.
(33) Yoon, J.; Choi, S.; Jin, S.; Jin, K. S.; Heo, K.; Ree, M. *J. Appl. Crystallogr.* **2007**, *40*, s669.
(34) Guo, J.; Liang, Y.; Szarko, J.; Lee, B.; Son, H. J.; Rolczynski, B. S.; Yu, L.; Chen, L. X. *J. Phys. Chem. B* **2010**, *114*, 4746.
(35) Reichenbaecher, K.; Suess, H. I.; Hulliger, J. *Chem. Soc. Rev.* **2005**, *34*, 22.
(36) Coffin, R. C.; Peet, J.; Rogers, J.; Bazan, G. C. *Nat. Chem.* **2009**, *1*, 657.
(37) Chen, M.-H.; Hou, J.; Hong, Z.; Yang, G.; Sista, S.; Chen, L.-M.; Yang, Y. *Adv. Mater.* **2009**, *21*, 4238.
(38) Nguyen, L. H.; Hoppe, H.; Erb, T.; Guenes, S.; Gobsch, G.; Sariciftci, N. S. *Adv. Funct. Mater.* **2007**, *17*, 1071.
(39) Mihailetchi, V. D.; Wildeman, J.; Blom, P. W. M. *Phys. Rev. Lett.* **2005**, *94*, 126602.
(40) Woo, C. H.; Thompson, B. C.; Kim, B. J.; Toney, M. F.; Frechet, J. M. J. *J. Am. Chem. Soc.* **2008**, *130*, 16324.
(41) Kline, R. J.; McGehee, M. D.; Kadnikova, E. N.; Liu, J.; Frechet, J. M. J. *Adv. Mater.* **2003**, *15*, 1519.
(42) Kline, R. J.; McGehee, M. D.; Kadnikova, E. N.; Liu, J.; Frechet, J. M. J.; Toney, M. F. *Macromolecules* **2005**, *38*, 3312.
(43) Ballantyne, A. M.; Chen, L.; Dane, J.; Hammant, T.; Braun, F. M.; Heeney, M.; Duffy, W.; McCulloch, I.; Bradley, D. D. C.; Nelson, J. *Adv. Funct. Mater.* **2008**, *18*, 2373.
(44) Moliton, A.; Nunzi, J.-M. *Polym. Int.* **2006**, *55*, 583.
(45) Potscavage, W. J., Jr.; Sharma, A.; Kippelen, B. *Acc. Chem. Res.* **2009**, *42*, 1758.
(46) Wei, G.; Wang, S.; Renshaw, K.; Thompson, M. E.; Forrest, S. R. *ACS Nano* **2010**, *4*, 1927.
(47) Coakley, K. M.; McGehee, M. D. *Chem. Mater.* **2004**, *16*, 4533.
(48) Miyanishi, S.; Tajima, K.; Hashimoto, K. *Macromolecules* **2009**, *42*, 1610.
(49) Nelson, J.; Kirkpatrick, J.; Ravirajan, P. *Phys. Rev. B* **2004**, *69*, 035337/1.
(50) Shuttle, C. G.; O'Regan, B.; Ballantyne, A. M.; Nelson, J.; Bradley, D. D. C.; Durrant, J. R. *Phys. Rev. B* **2008**, *78*, 113201/1.
(51) Vandewal, K.; Tvingstedt, K.; Gadisa, A.; Inganaes, O.; Manca, J. V. *Nat. Mater.* **2009**, *8*, 904.
(52) Andrea Maurano, R. H.; Shuttle, C. G.; Ballantyne, A. M.; Nelson, J.; O'Regan, B.; Zhang, W.; McCulloch, I.; Azimi, H.; Morana, M.; Brabec, C. J.; Durrant, J. R. *Adv. Mater.* **2010**, *22*, 4987.
(53) Abdou, M. S. A.; Holdcroft, S. *Macromolecules* **1993**, *26*, 2954.
(54) Rabek, J. F. *Mechanisms of photophysical processes and photochemical reactions in polymers: Theory and application*; John Wiley & Sons: New York, 1987.
(55) Jensen Rasmus, L.; Arnbjerg, J.; Ogilby Peter, R. *J. Am. Chem. Soc.* **2010**, *132*, 8098.
(56) Scurlock, R. D.; Wang, B.; Ogilby, P. R.; Sheats, J. R.; Clough, R. L. *J. Am. Chem. Soc.* **1995**, *117*, 10194.
(57) Gorman, A. A.; Hamblett, I.; Smith, K.; Standen, M. C. *Tetrahedron Lett.* **1984**, *25*, 581.
(58) D'Auria, M.; Ferri, R. *J. Photochem. Photobiol. A* **2003**, *157*, 1.
(59) Frimer, A. A. *Singlet O2*; CRC Press: Boca Raton, 1985; Vol. 2, Reaction Modes and Products Part 1.
(60) Kopecky, J. *Organic photochemistry: A visual approach*; VCH Publishers: New York, 1992.
(61) Shrotriya, V.; Li, G.; Yao, Y.; Moriarty, T.; Emery, K.; Yang, Y. *Adv. Funct. Mater.* **2006**, *16*, 2016.